ScienceDirect

ELSEVIER

Electrochimica Acta 52 (2007) 5095–5101

Acta

www.elsevier.com/locate/electacta

PEM fuel cells operated at 0% relative humidity in the temperature range of 23–120 °C

Jianlu Zhang, Yanghua Tang, Chaojie Song, Xuan Cheng [1], Jiujun Zhang [*,2], Haijiang Wang

Institute for Fuel Cell Innovation, National Research Council of Canada, Vancouver, BC, Canada V6T 1W5

Received 15 October 2006; received in revised form 8 February 2007; accepted 8 February 2007
Available online 13 February 2007

Abstract

Operation of a proton exchange membrane (PEM) fuel cell without external humidification (or 0% relative humidity, abbreviated as 0% RH) of the reactant gases is highly desirable, because it can eliminate the gas humidification system and thus decrease the complexity of the PEM fuel cell system and increase the system volume power density (W/l) and weight power density (W/kg). In this investigation, a PEM fuel cell was operated in the temperature range of 23–120 °C, in particular in a high temperature PEM fuel cell operation range of 80–120 °C, with dry reactant gases, and the cell performance was examined according to varying operation parameters. An ac impedance method was used to compare the performance at 0% RH with that at 100% RH; the results suggested that the limited proton transfer process to the Pt catalysts, mainly in the inonomer within the membrane electrode assembly (MEA) could be responsible for the performance drop. It was demonstrated that operating a fuel cell using a commercially available membrane (Nafion® 112) is feasible under certain conditions without external humidification. However, the cell performance at 0% RH decreased with increasing operation temperature and reactant gas flow rate and decreasing operation pressure.

Keywords: PEM fuel cells; High temperature; Dry reactant gas (or 0% relative humidity); External humidification

1. Introduction

In recent years, tremendous effort in the research and development of proton exchange membrane fuel cells (PEMFCs) has been concentrated on increasing power density, reducing cost, and improving reliability and durability [1]. Operation of PEMFCs at high temperatures (>80 °C) is considered an effective way to improve performance in terms of reaction kinetics, catalyst tolerance, heat rejection, and water management [2–13]. Therefore, high-temperature PEM fuel cells are considered to be the next generation of fuel cells.

With respect to water management, when using Nafion-based membranes such as Nafion 112, a high relative humidity (RH > 80%) is still required in order to obtain a practical performance, even when the fuel cell is operated at high temperatures. This is limited primarily by the low conductivity of the proton exchange membranes at elevated temperature, mainly induced by a low water content. Thus, an external humidification subsystem is required to ensure water retention in the membrane electrode assembly (MEA). Such a humidifier, which requires both space and a heat supply, causes a drop in system efficiency and is thus a burden to the fuel cell system. Therefore, system simplification is considered to be an important approach in the effort to increase power density. In particular, RH reduction in the feed air and hydrogen streams is believed to be an effective way to simplify the system [14,15].

The following approaches have been proposed to simplify or eliminate the external humidification subsystem in order to allow fuel cells to operate with less wet or dry reactant gases: (i) make self-humidifying membranes by incorporating Pt or metal-oxide particles into their structures [16–23]; (ii) input water through wicks or hollow fibers [14,23]; (iii) the design of special flow fields [24–27] and catalyst layers [28]. These work have made great progresses in terms of practical feasibility of low/0% RH operation and fundamental understanding. How-

* Corresponding author. Tel.: +1 604 221 3087; fax: +1 604 221 3001.
E-mail address: jiujun.zhang@nrc.gc.ca (J. Zhang).
[1] Permanent address: Department of Materials Science and Engineering, State Key Laboratory for Physical Chemistry of Solid Surfaces, Xiamen University, Xiamen FJ 361005, PR China.
[2] Active member of the International Society of Electrochemistry.

0013-4686/$ – see front matter © 2007 Elsevier Ltd. All rights reserved.
doi:10.1016/j.electacta.2007.02.002

ever, there are still some challenges with respect to the strategies of self-humidifying membranes, embedding Pt particles in the membranes, and designing alternative flow field structures.

The ideal situation is to operate a PEMFC at 0% RH. The feasibility of doing this has been investigated through a number of approaches and corresponding theories or models. Bernardi and Verbrugge [29] pointed out that in a broad range of practical current densities, there are no external water requirements because the water produced at the cathode is sufficient to meet the water requirement of a membrane in a fuel cell. Therefore, it is feasible to operate a fuel cell without external humidification, relying only on the water produced at the cathode by electrochemical reaction. Recently, there have been several reports regarding the water transport in a PEM fuel cell without external humidification [30–44]. The experimental results showed that the cell performance under dry conditions was strongly dependent on the cell's operating temperature [27,30,35,40], flow field design [27,30,40,43], electrode area as well as preparation procedure [30], and the inlet gas stoichiometric flow rates [35,36,44].

In this study, the performance of a PEM fuel cell operated with dry hydrogen and air was investigated in the temperature range of 23–120 °C. It is believed that this wide temperature range, especially the range of 80–120 °C, may be more important in terms of the performance improvement mentioned above. An ac impedance method was used to diagnose the loss of fuel cell performance at 0% RH. The effects of operation temperature, feed gas flow rate, and backpressure were also studied. The results indicated that the operation of a PEMFC at 0% RH using a typical, commercially available membrane (Nafion 112) is feasible at a wide temperature range.

2. Experimental

The membrane electrode assembly (MEA), with an active area of 4.4 cm^2, was prepared by hot pressing the anode, a Nafion 112 membrane, and cathode together at 135 °C and 75 kg/cm^2 for 2 min. The gas diffusion electrode (GDE) was prepared by spraying a homogeneous catalyst ink, consisting of catalyst, Nafion® solution and iso-propanol, onto a gas diffusion layer (GDL). This GDL was a PTFE and carbon black impregnated carbon paper (Toray, TGP-H-060). E-Tek 20% Pt/Ru/C and 40% Pt/C were used as the anode and cathode catalysts, respectively with a total Pt loading of ~1.0 mg/cm^2. The total Nafion loading in the MEA was 1.4 mg/cm^2. The Nafion® 112 (DuPont), used for the proton electrolyte membrane, was treated in 3% H_2O_2(aq), 1 M H_2SO_4(aq); rinsed; then soaked separately in deionized water for 1 h at 60–80 °C, followed by a careful washing with double-distilled water.

The MEA was tested in an in-house single cell fed with dry H_2 and air at different operating conditions, such as relative humidities, and gas flow rates (or stoichiometries). The gas flow rates presented in this paper were the mass flow rates at standard condition (1 atm, 0 °C). A 100 Fideris fuel cell 100 W test station controlled by FC Power software, and equipped with an in-house modified humidifier which could reach 100% RH at 120 °C, was used for the tests. The single fuel cell hardware was the same as described in Ref. [45]. A bladder pressure of 4.4 atm was used to hold the single cell together and provide sufficient electrical contact between the MEA and the graphite bipolar plates. Both graphite plates had the same serpentine flow fields. When the cell was operated at 100% RH, before H_2 and air were fed into the anode and cathode, they were first passed through their corresponding humidifiers, where they were humidified at the same temperature as that of the operating cell. When the cell was operated at 0% RH, the dry gases were fed directly into the single cell. Polarization data were collected at different temperatures and backpressures (1.0, 2.0 and 3.0 atm absolute) were controlled by the test station, and the cell voltage under each current density was recorded after the reading was stable. During all tests, the pressures for both anode and cathode side were kept at the same level.

A Solartron 1260 FRA was used for ac impedance measurements in the frequency range of 10,000–0.01 Hz, using a method described in our previous paper [45]. The purpose of ac impedance experiments is to obtain the membrane resistance, electrode kinetic, and mass transfer resistances of the fuel cell reactions.

3. Results and discussion

3.1. Background of water balance in a fuel cell without external humidification

For a PEM fuel cell operated with dry reactant gases, the water sources are that produced by the electrochemical reduction of oxygen at the cathode ($O_2 + 4H^+ + 4e^- \Rightarrow 2H_2O$). Note that the direct chemical reaction of O_2 (or H_2) with H_2 (or O_2) crossed over through the membrane could also make a contribution to the water quantity. However, the water produced by this chemical reaction is much less than that produced by the electrochemical reduction of oxygen. Therefore the water produced by the electrochemical reduction of oxygen at the cathode is considered as the only water source in this paper. The process can be expressed schematically as shown in Fig. 1. Due to the water production and accumulation in the cathode, a water concentration gradient between the cathode and anode is generated. This gradient drives a water crossover through the membrane from cathode to anode. This process is called *back diffusion* [32]. The back-diffused water humidifies the hydrogen stream in the anode side. The superfluous humidified hydrogen then flows out as exhausted or recycling gas. However, due to the current flows in the fuel cell, protons transport across the mem-

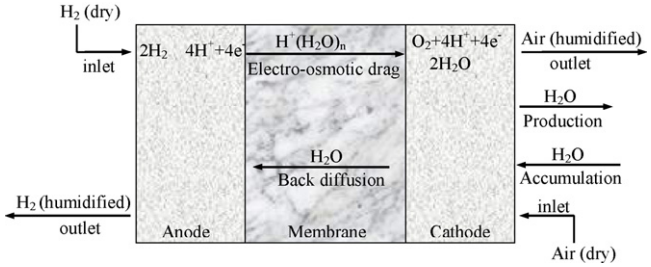

Fig. 1. Schematic illustration of water transport modes in MEA without external humidification.

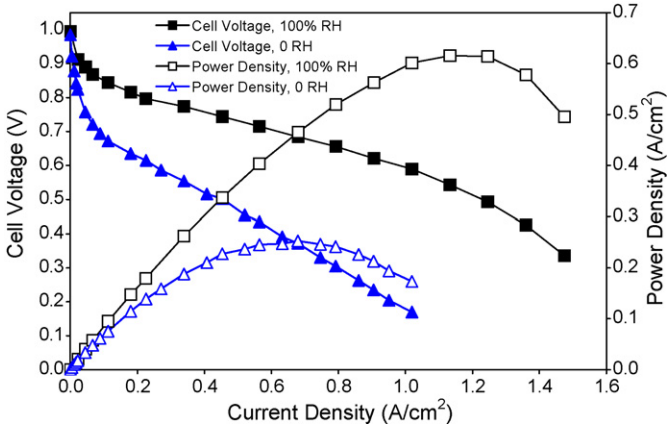

Fig. 2. Cell voltage and power density as a function of current density. Single fuel cell with an active MEA area of 4.4 cm^2 operated at 80 °C, 3.0 atm absolute backpressure, 100% RH and 0% RH. The stoichiometries of H_2 and air are 1.5 and 2.0, respectively. Standard MEA with Nafion 112 membrane and a total Pt loading of 1.0 mg/cm^2.

brane from anode to cathode and carry some water molecules. This process is called *electro-osmotic drag* and has been treated by a solution water diffusion model [46–48] and a convective water transport model [49]. The drag coefficient, H_2O/H^+ (the number of water molecules moving with each H^+ in the absence of concentration gradients), is about 1.0 and 2.5 for a vapour-equilibrated and a liquid-equilibrated membrane, respectively [50]. Electro-osmotic drag and back diffusion balance the water in the MEA and keep the membrane hydrated. At high temperature, water vaporization is expected to have a strong influence on the water balance in a fuel cell.

3.2. Cell performance without external humidification

Fig. 2 shows the PEM fuel cell performance at 80 °C, 3.0 atm absolute. Performance with dry H_2 and air is compared with performance with fully humidified H_2 and air. At 0% RH, a maximum MEA power density of 0.25 W/cm^2 could be obtained, indicating that the fuel cell can be operated at such extreme conditions and the membrane can be self-humidified by the water produced in cathode. This power density at 0% RH represents 40% of the performance of 0.62 W/cm^2 for 100% RH operation.

In more detailed analysis, a significant performance drop at 0% RH, compared with that obtained at 100% RH, was diagnosed by an *in situ* ac impedance method developed in-house [45]. Fig. 3(a) shows the obtained spectra at 100% RH. Basically two semicircles can be observed on each spectrum, one in the high frequency domain and the other in the low frequency domain. Similar spectra have been widely reported in the literature for PEM fuel cells [51–53]. The intercept in the high frequency domain on the Z' axis of Fig. 3(a) represents the membrane resistance from which the membrane through-plane conductivity in real fuel cell operating conditions can be measured. The first semicircle represents fuel cell reaction kinetics, with the contributions coming from the cathodic oxygen reduction process and the anodic hydrogen oxidation (mainly dominated by oxygen reduction reaction). The second semicircle represents the mass transfer process, with the contributions coming from the diffusion of reactants within the membrane (proton diffusion) to the Pt active surface within the cathodic (oxygen) and anodic (hydrogen) catalyst layers.

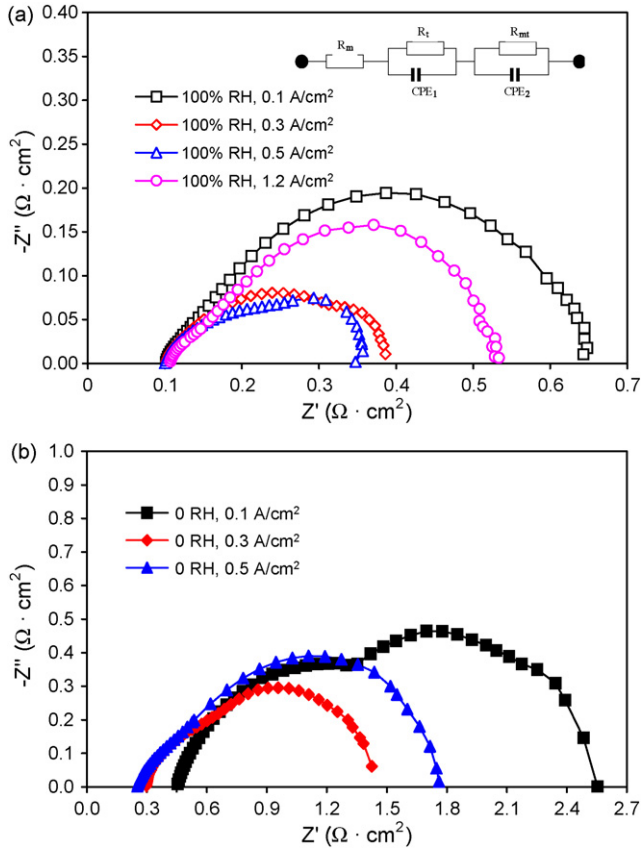

Fig. 3. *In situ* ac impedance spectra at the frequency range of 10,000–0.01 Hz. Single fuel cell with an active MEA area of 4.4 cm^2 operated at 80 °C, 3.0 atm absolute backpressure: (a) 100% RH (b) 0% RH. The stoichiometries of H_2 and air are 1.5 and 2.0, respectively. Standard MEA with Nafion 112 membrane and a total Pt loading of 1.0 mg/cm^2.

In the case of 100% RH, the mass transfer process could be dominated by oxygen diffusion at the cathodic catalyst layer. At low current load (0.1 A/cm^2), the semicircle is dominated mainly by a high-frequency semicircle, indicating that the reaction process was limited by the kinetics. At high current loads (1.2 A/cm^2), the second, lower frequency semicircle dominates, suggesting that the reaction process was limited by the mass transfer within the catalyst layer.

It can be observed in Fig. 3(a) that the first semicircle shrinks and the second semicircle expands with increasing current. This behaviour has been observed widely in the research for PEM fuel cell ac impedance spectra [51,52,54]. An equivalent circuit was constructed to describe the process, as shown in the insert in Fig. 3(a). R_m is the high-frequency resistance (intercept on Z' axis at the high frequency end), which represents the membrane resistance. R_t is the charge transfer resistance for oxygen reduction, and CPE_1 (constant phase element) represents the R_t associated catalyst layer capacitance properties. R_{mt} is the resistance related to the mass transfers of reactants (O_2, H_2, and/or H^+) within the membrane electrode assembly. CPE_2 represents

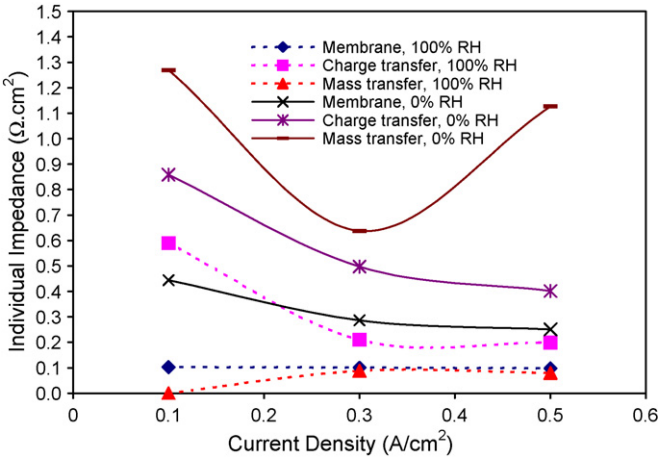

Fig. 4. Simulated individual ac impedances as a function of current density. The simulation was based on the data in Fig. 3 according to the equivalent circuit in Fig. 3(a).

the R_{mt} associated capacitance. For a detailed explanation of CPE, please see Ref. [55]. The equivalent circuit in Fig. 3(a) was used to simulate the impedance data by *Z*-plot, as discussed later in this paper.

Fig. 3(b) shows the ac impedance spectra at 0% RH. Again, two semicircles can be observed, representing the charge transfer and mass transfer resistances. The simulated individual impedance values according to the equivalent circuit in Fig. 3(a) were plotted as a function of current density, as shown in Fig. 4. Compared to the resistance values at 100% RH, the membrane, charge transfer, and mass transfer resistances all jumped dramatically, suggesting that all of these processes together are responsible for the performance drop at 0% RH.

At 0% RH, the membrane and the ionomer inside the catalyst layer were dry (much less water content than that at 100% RH), resulting in a 4.5–2.8 times higher proton conduction resistance than that at 100% RH in the current density range of 0.1–0.5 A/cm^2 (Fig. 4). In a dry membrane or ionomer medium, the proton transport became difficult because not enough water was available for proton osmotic drag [56]. This dry environment could also slow down the charge transfer process, as evidenced by the 1.5–2.0 times higher charge transfer resistance than that at 100% RH. This could be due to the reduction of electrochemical Pt surface area in the dry catalyst layers [16,25,32,57].

In Fig. 4, the most predominant resistance jump is the mass transfer resistance. At 0.1 A/cm^2, a jump from 0 at 100% RH to a value of 1.27 Ω cm^2 at 0% RH can be observed. At 0.3 A/cm^2, because more water was produced, the jump was smaller (from 0.09 to 0.69 Ω cm^2). However, when the current density increased to 0.5 A/cm^2, the mass transfer resistance jump became large again, from 0.08 to 1.13 Ω cm^2. It is unlikely that the larger jump of mass transfer resistance at 0.1 A/cm^2 came from the oxygen or hydrogen transportation limitation because the reaction stoichiometries for hydrogen and oxygen were high enough, respectively. This large mass transfer resistance at 0% RH may be interpreted as the limited proton transfer process to the Pt catalysts, mainly in the inonomer within a dry MEA. When the current density was increased to 0.3 A/cm^2, more water was produced, generating a slightly improved wet environment within the MEA. In this case, the proton transportation improved, resulting in a smaller mass transfer resistance. However, when the current density was further increased to 0.5 A/cm^2, even more water was produced and the demand for water for proton osmotic drag was increased at the same time. Therefore, the large mass transfer resistance increase is still believed to be from the proton transportation limitation within the catalyst layers. In summary, the large mass transfer resistance increase observed at 0% RH could be explained according to the limited proton transfer process to the Pt catalysts, mainly in the inonomer within a dry MEA environment.

In the following section, the effects of operation parameters on the water balance in the MEA and cell performance in a PEM fuel cell operated at 0% RH are briefly discussed, based on the experiment results.

3.3. Effect of operation temperature

Operation temperature is expected to affect cell performance more significantly in dry reactant gas conditions by changing the water balance and reaction kinetics in the fuel cell. Increased temperature can accelerate water evaporation, resulting in a reduction of water retention. This has a negative impact on the cell performance. However, increased temperature can also increase the kinetics of both oxygen reaction and hydrogen oxidation reactions, resulting in a higher performance. There should be a trade-off between water retention and reaction kinetics.

As shown in Fig. 5, at 23 and 60 °C, the cell performances were almost the same at low current density (below 0.3 A/cm^2), with a higher performance at 60 °C in the high current density range. The water retention in MEA was stronger at 23 °C than at 60 °C, but the kinetics was slower at 23 °C than at 60 °C. The trade-off between water retention and kinetics may be responsible for the similar performances in the low current density range. At higher current densities, the positive impact of accelerated reaction kinetics at 60 °C on the performance

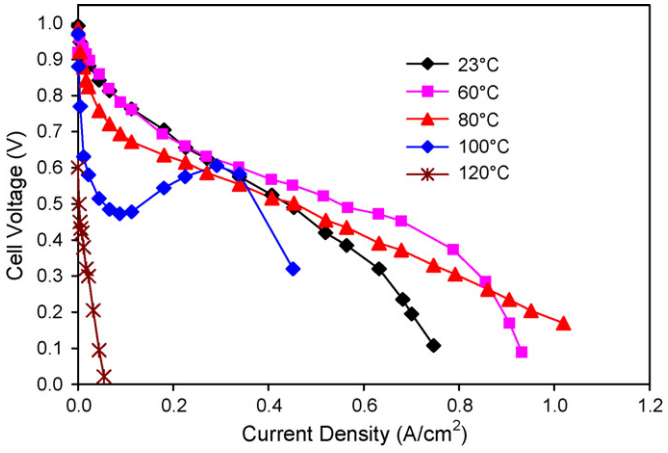

Fig. 5. Cell voltages as a function of current density at different temperatures. Single fuel cell with an active MEA area of 4.4 cm^2 operated at 3.0 atm absolute backpressure and 0% RH. The stoichiometries of H_2 and air are 1.5 and 2.0, respectively. Standard MEA with Nafion 112 membrane and a total Pt loading of 1.0 mg/cm^2.

may overwhelm the negative impact of less water retention, resulting in higher performance.

Further increasing the operation temperature to 80 °C lowered the cell performance, and for temperatures over 80 °C, performance dropped dramatically. This is mainly because the water retention became a problem even though the reaction kinetics is faster than at lower temperatures. The water more easily vaporizes at high temperatures (above 80 °C) than at low temperatures. Therefore, less water was retained in the MEA and very little water could be back diffused from cathode to anode, so the activity of protons in the anode was very low. In this case the membrane was dehydrated since the produced water could not humidify it sufficiently, which led to decreases in proton conductivity and performance.

It is worth noting that there was a jump of cell performance at 100 °C when the current density was higher than 0.1 A/cm^2. This is because the amount of water produced was more than that evaporated. The leftover water started to humidify the membrane and back-diffused to the anode for proton transportation.

This result clearly indicates that a fuel cell can be operated at 100 °C without an external humidifier. However, when temperature goes up to 120 °C, the current density is limited, primarily by the proton transportation. Such low current density cannot produce enough water for water balance, resulting in a much poor performance.

3.4. Effect of operation pressure

The effect of operation pressure on cell performance is shown in Fig. 6. The cell performance decreased with decreasing backpressure. Decreasing backpressure has two negative impacts on performance. The first is the partial pressure drop of hydrogen and oxygen at low operation pressure. The second is the increase in the volume flow rate of reactant gas with the reduction of operation pressure when the mass flow rate is constant. The water retained in both the cathode and the anode is more readily purged by their respective gas streams with a high volume flow rate than with a low one. Therefore the membrane is more easily dehydrated, and thus the cell performance decreases at a lower operation backpressure. A similar trend was also observed on the fuel cell operated at the temperature range of 80–120 °C (not shown here).

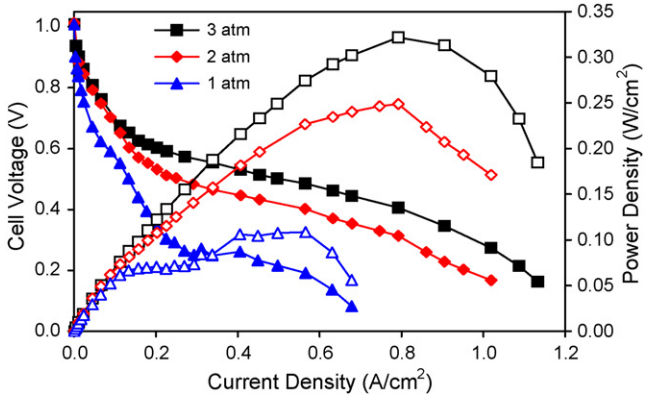

Fig. 6. Cell voltages as a function of current density at different backpressures. Single fuel cell with an active MEA area of 4.4 cm^2 operated at 23 °C and 0% RH. Air flow rate, 1000 ml/min; hydrogen flow rate, 750 ml/min. Standard MEA with Nafion 112 membrane and a total Pt loading of 1.0 mg/cm^2.

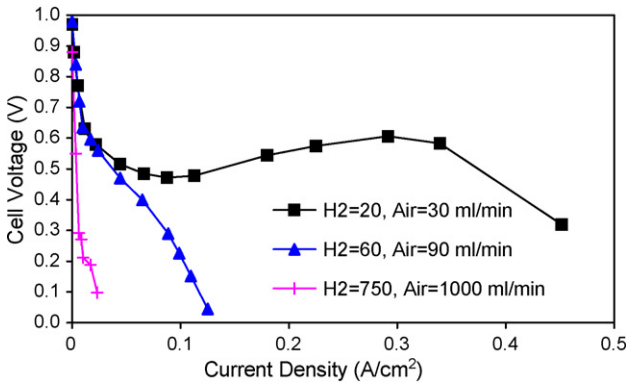

Fig. 7. Cell voltages as a function of current density at different gas flow rates. Single fuel cell with an active MEA area of 4.4 cm^2 operated at 100 °C, 3.0 atm absolute, and 0% RH. Standard MEA with Nafion 112 membrane and a total Pt loading of 1.0 mg/cm^2.

3.5. Effect of gas reactant flow rate

The effect of reactant gas flow rate at 100 °C on cell performance is shown in Fig. 7. The cell performance decreased with an increase in gas flow rates. As discussed above, both higher temperature and higher gas flow rate favour the removal of water from MEA and the transport of water in the MEA. Thus, too much water was brought out with the outlet streams and water retention became a problem for membrane humidification. Consequently, the membrane became increasingly dry with the increase in gas flow rate. This trend is more obvious at 100 °C, as shown in Fig. 7. A similar trend was also observed on the fuel cell operated at 80 and 120 °C (not shown here).

3.6. Dynamic behaviour of the performance

Fig. 8 shows the cell voltage and the current change as a function of polarization time during the 0% RH operation at

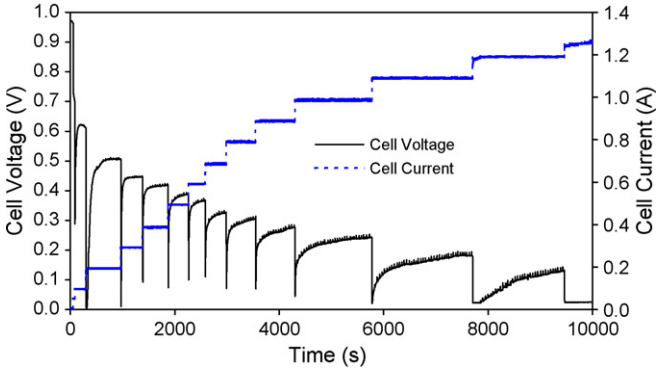

Fig. 8. Cell voltage and current density as a function of polarization time at 80 °C, 3.0 atm absolute with dry H_2 and air. The flow rates of H_2 and air were 750 and 1000 ml/min, respectively. Single fuel cell with an active MEA area of 4.4 cm^2. Standard MEA with Nafion 112 membrane and a total Pt loading of 1.0 mg/cm^2.

80 °C, 3.0 atm (absolute) with dry H_2 and air. As can be seen, the cell voltage varied periodically with time upon current steps, suggesting that the performance of the cell depends on the equilibration time [30,34]. When the current increased, the voltage dropped dramatically to a very low level (bottom level), and then increased slowly with time. This can be interpreted as being due to the water transportation in the MEA. With an increase in current, more protons were required to transport from the anode to the cathode; however, the proton activity remained low since not enough water was available in the anode. At this stage, the proton transportation was the limiting step. In order to maintain the current density, more electrode polarizations were needed, resulting in a bottom cell voltage. With constant water production and accumulation in the cathode, a larger water concentration gradient was formed, which accelerated the water transportation from the cathode to the anode and the hydration of the membrane. Thus, the cell voltage increased with time and reached a stable value gradually. It was also noted that the equilibration time got longer with the increase of current, especially at high current domain, because it needed longer to produce enough water to hydrate the membrane.

4. Conclusions

The operation of a Nafion 112-based PEM fuel cell without external humidification of the reactant gases was demonstrated and investigated in the temperature range of 23–120 °C. The performance at 0% RH was much lower than that at 100% RH. The ac impedance method was used to diagnose the performance drop. It is believed that the major cause of lower performance was the slow proton transportation within the catalyst layers. It was suggested that it is feasible to operate a fuel cell using a commercially available Nafion-based membrane without external humidification. However, the cell performance was strongly dependent on the operation temperature, backpressure, and reactant gas flow rate. According to preliminary results presented in this paper, a low gas flow rate (or stoichiometry) and a high backpressure (>ambient pressure) are beneficial to operating a commercially available Nafion 112-based PEM fuel cell at 0% RH.

The influence of water balance in the PEM fuel cell operated at 0% RH due to the change of operation parameters was briefly discussed. Further investigation was undertaken to provide more systematic and quantitative analysis with respect to the water balance and cell performance.

Acknowledgements

The authors would like to thank the financial support of the NRC National PEM Fuel Cell Program and the NRC Institute for Fuel Cell Innovation. Dr. Xuan Cheng also greatly appreciates the financial supports from the China Scholarship Council and the National Natural Science Foundation of China (20433060) for the living allowances during her visit and stay at NRC-IFCI. The authors also thank Mr. Ryan Baker for his help in the editing.

References

[1] J. Larminie, A. Dicks, Fuel Cell Systems Explained, 2nd ed., John Wiley & Sons, Chichester, England, 2000.
[2] P. Costamagna, S. Srinivasan, J. Power Sources 102 (2001) 242.
[3] P. Costamagna, S. Srinivasan, J. Power Sources 102 (2001) 253.
[4] R.K. Ahluwalia, E.D. Doss, R. Kumar, J. Power Sources 117 (2003) 45.
[5] K.T. Adjemian, S.J. Lee, S. Srinivasan, J. Benziger, A.B. Bocarsly, J. Electrochem. Soc. 149 (2002) A256.
[6] Y.-T. Kim, M.-K. Song, K.-H. Kim, S.-B. Park, S.-K. Min, H.-W. Rhee, Electrochim. Acta 50 (2004) 645.
[7] V. Ramani, H.R. Kunz, J.M. Fenton, J. Membr. Sci. 232 (2004) 31.
[8] C. Yang, P. Costamagna, S. Srinivasan, J. Benziger, A.B. Bocarsly, J. Power Sources 103 (2001) 1.
[9] S. Malhotra, R. Datta, J. Electrochem. Soc. 144 (1997) L23.
[10] Z. Qi, C. He, A. Kaufman, J. Power Sources 111 (2002) 239.
[11] H. Xu, Y. Song, H.R. Kunz, J.M. Fenton, J. Electrochem. Soc. 152 (2005) A1828.
[12] A. Parthasarathy, S. Srinivasan, A.J. Appleby, J. Electrochem. Soc. 139 (1992) 2530.
[13] Y. Song, J.M. Fenton, H.R. Kunz, L.J. Bonville, M.V. Williams, J. Electrochem. Soc. 152 (2005) A539.
[14] S.-H. Ge, X.-G. Li, I.-M. Hsing, J. Electrochem. Soc. 151 (2004) B523.
[15] Y. Cai, J. Hu, H. Ma, B. Yi, H. Zhang, Electrochim. Acta 51 (2006) 6361.
[16] M. Watanabe, H. Uchida, M. Emori, J. Phys. Chem. B 102 (1998) 3129.
[17] H. Uchida, Y. Ueno, H. Hagihara, M. Watanabe, J. Electrochem. Soc. 150 (2003) A57.
[18] F. Liu, B. Yi, D. Xing, J. Yu, Z. Hou, Y. Fu, J. Power Sources 124 (2003) 81.
[19] S.H. Kwak, T.H. Yang, C.S. Kim, K.H. Yoon, J. Power Sources 118 (2003) 200.
[20] M. Watanabe, H. Uchida, Y. Seki, M. Emori, P. Stonehart, J. Electrochem. Soc. 143 (1996) 3847.
[21] T.H. Yang, Y.G. Yoon, C.S. Kim, S.H. Kwak, K.H. Yoon, J. Power Sources 106 (2002) 328.
[22] B. Yang, Y.Z. Fu, A. Manthiram, J. Power Sources 139 (2005) 170.
[23] M. Watanabe, Y. Satoh, C. Shimura, J. Electrochem. Soc. 140 (1993) 3190.
[24] A. Kaufmann, P.L. Terry, US Patent No. 5,776,725, 1998.
[25] Z. Qi, A. Kaufmann, J. Power Sources 109 (2002) 469.
[26] K. Tuber, M. Zobel, H. Schmidt, C. Hebling, J. Power Sources 122 (2003) 1.
[27] W.H.J. Hogarth, J.B. Benziger, J. Power Sources 159 (2006) 968.
[28] U.H. Jung, K.T. Park, E.H. Park, S.H. Kim, J. Power Sources 159 (2006) 529.
[29] D.M. Bernardi, M.W. Verbrugge, J. Electrochem. Soc. 139 (1992) 2477.
[30] N. Rajalakshmi, T.T. Jayanth, R. Thangamuthu, G. Sasikumar, P. Sridhar, K.S. Dhathathreyan, Int. J. Hydrogen Energy 29 (2004) 1009.
[31] D.R. Sena, E.A. Ticianelli, V.A. Paganin, E.R. Gonzalaez, J. Electroanal. Chem. 477 (1999) 164.
[32] F.N. Buchi, S. Srinivasan, J. Electrochem. Soc. 144 (1997) 2767.
[33] F.N. Buchi, D. Tran, S. Srinivasan, Proc. Electrochem. Soc. (1995) 95–23 (proton conducting membrane fuel cells I) 226–240.
[34] S. Srinivasan, S. Gamburzev, O.A. Velev, F. Simoneaux, A.J. Appleby, Fuel Cell Seminar—Program and Abstracts, Washington, DC, 1996, pp. 513–516.
[35] A. Su, C.C. Sun, F.B. Weng, Y.M. Chen, Exp. Heat Transf. 16 (2003) 97.
[36] M.V. Williams, H.R. Kunz, J.M. Fenton, J. Power Sources 135 (2004) 122.
[37] S.H. Chan, S.K. Goh, S.P. Jiang, Electrochim. Acta 48 (2003) 1905.
[38] D. Picot, R. Metkmeijer, J.J. Bezian, L. Rouveyre, J. Power Sources 75 (1998) 251.
[39] M. Hsing, P. Futerko, Chem. Eng. Sci. 55 (2000) 4209.
[40] M. Noponen, T. Mennola, M. Mikkola, T. Hottinen, P. Lund, J. Power Sources 106 (2002) 304.
[41] G. Faita, A. Toro, L. Merlo, Z.Y. Xue, WO 2005060031 A2, 2005.
[42] A. Toro, WO 2006053767 A1, 2006.
[43] W.H.J. Hogarth, J.B. Benziger, J. Electrochem. Soc. 153 (2006) A2139.
[44] H. Yu, C. Ziegler, J. Electrochem. Soc. 153 (2006) A570.

[45] Y. Tang, J. Zhang, C. Song, H. Liu, J. Zhang, H. Wang, S. Mackinnon, T. Peckham, J. Li, S. McDermid, P. Kozak, J. Electrochem. Soc. 153 (2006) A2036.
[46] T.E. Springer, T.A. Zawodzinski, S. Gottesfeld, J. Electrochem. Soc. 138 (1991) 2334.
[47] T.V. Nguyen, R.E. White, J. Electrochem. Soc. 140 (1993) 2178.
[48] T. Okada, J. Elecroanal. Chem. 465 (1999) 18.
[49] M. Eikerling, Y.I. Kharkats, A.A. Kornyshev, Y.M. Volfkavich, J. Electrochem. Soc. 145 (1998) 2684.
[50] T.A. Zawodzinski, J. Davey, J. Valerio, S. Gottesfeld, Electrochim. Acta 40 (1995) 297.
[51] T.E. Springer, T.A. Zawodzinski, M.S. Wilson, S. Gottesfeld, J. Electrochem. Soc. 143 (1996) 587.
[52] T.J.P. Freire, E.R. Gonzalez, J. Electroanal. Chem. 503 (2001) 57.
[53] V.A. Paganin, C.L.F. Oliveira, E.A. Tocianelli, T.E. Springer, E.R. Gonzalez, Electrochim. Acta 43 (1998) 3761.
[54] K. Wiezell, P. Gode, G. Lindbergh, J. Electrochem. Soc. 153 (2006) A749.
[55] G.J. Brug, A.L.G. Van Den Eeden, M. Sluyters-Rehbach, J.H. Sluyters, J. Electroanal. Chem. 176 (1984) 275.
[56] A.V. Anantaraman, C.L. Gardner, J. Electroanal. Chem. 414 (1996) 115.
[57] C. Song, J. Zhang, Y. Tang, J. Zhang, H. Wang, J. Li, S. McDermid, P. Kozak, Electrochim. Acta 52 (2007) 2552.